International Journal of Modern Physics E
Vol. 27, No. 10 (2018) 1850089 (13 pages)

DOI: 10.1142/S0218301318500891

Investigation of the elastic and inelastic scattering of ^{3}He from ^{9}Be in the energy range 30–60 MeV

D. M. Janseitov[*,†,¶,‖], S. M. Lukyanov[*,**], K. Mendibayev[*,†,§],
Yu. E. Penionzhkevich[*,‡], N. K. Skobelev[*], Yu. G. Sobolev[*],
K. A. Kuterbekov[§], D. S. Valiolda[¶] and T. K. Zholdybayev[†]

[*]*Joint Institute for Nuclear Research,*
Joliot-Curie 6, 141980 Dubna, Russian Federation

[†]*Institute of Nuclear Physics,*
Ibragimov 1, 050032 Almaty, Republic of Kazakhstan

[‡]*National Research Nuclear University MEPhI,*
Kashirskoe shosse 31, 1115409 Moscow, Russian Federation

[§]*L. N. Gumilyov Eurasian National University,*
Satpayev 2, 010008 Astana,
Republic of Kazakhstan

[¶]*al-Farabi Kazakh National University,*
al-Farabi 71, 050040 Almaty, Republic of Kazakhstan
[‖]*janseit.daniar@gmail.com*
[**]*lukyan@jinr.ru*

W. H. Trzaska, S. V. Khlebnikov and G. P. Tyurin

Department of Physics, University of Jyväskylä,
Seminaarinkatu 15, FI-40014 Jyväskylä, Finland

B. A. Urazbekov

Department of Mathematics and Physics,
Universita degli studi della Campania Luigi Vanvitelli,
Viale Lincoln 5, 81100 Caserta, Italy

M. N. Harakeh

KVI-CART, University of Groningen,
Zernikelaan 25, 9747 AA Groningen, The Netherlands

V. Burjan, V. Kroha, J. Mrazek, Š. Piskoř, I. Sivaček and V. Glagolev

Nuclear Physics Institute, 250068 Řež, Czech Republic

Received 3 August 2018
Revised 23 October 2018
Accepted 25 October 2018
Published 12 November 2018

We have measured the differential cross-sections for the elastic as well as inelastic scattering populating the 2.43 MeV ($5/2^-$) excited state in ^{9}Be using ^{3}He beams at energies of 30, 40 and 47 MeV on a ^{9}Be target. The experimental results for the elastic scattering were analyzed within the framework of the optical model using the Woods–Saxon and double-folding potentials. The theoretical calculations for the concerned excited states were performed using the coupled-channel method. The optimal deformation parameters for the excited states of ^{9}Be nucleus were extracted.

Keywords: Elastic scattering; inelastic scattering; coupled-channel methods; deformation parameters.

PACS Number(s): 21.60.Gx, 24.10 Ht, 25.55.Ci

1. Introduction

The study of elastic and inelastic processes of interaction of helium isotopes ^{3,4}He with nuclei is one of the main sources of information on the properties of the ground and low-lying excited states of atomic nuclei. These processes, which occur in the collisions of helium isotopes ^{3,4}He with energies of several tens of MeV, make it possible to obtain valuable information on the structure of specific nuclear states. Of particular interest in this respect it is the structural feature of the ^{9}Be nucleus. The ^{9}Be nucleus is a unique example of a nuclear system that exhibits a cluster structure while remaining a stable but weakly bound nucleus. For example, the ^{9}Be nucleus can be considered as a core with the so-called Borromean structure: it can be represented as a configuration of three particles $\alpha + \alpha + \mathrm{n}$ (the 1n separation energy is -1.664 MeV), for which the removal of any one of the three constituents results in an unbound two-body subsystem.

In addition, it was suggested[1] that the state 1.68 MeV ($1/2^+$) in ^{9}Be has a neutron halo. Until now, the neutron halo has been observed almost exclusively in the ground states of some radioactive nuclei; detection of the neutron halo in stable light nuclei (e.g., ^{9}Be and ^{13}C) significantly expanded the prevailing ideas about nuclear exotics.[2,3] But, nevertheless, the ^{9}Be nucleus is one of the least studied 1p-shell nuclei. Several papers have reported investigations on elastic and inelastic scattering of deuterons and α particles on ^{9}Be. For example, in the following papers,[4,5] the processes of interaction of deuterons[4] and α particles[5] with ^{9}Be nuclei were analyzed using distorted-wave Born approximation (DWBA) and coupled-channel (CC) models with phenomenological potentials. Later, certain excited states of ^{9}Be were analyzed in the framework of the CC method with both phenomenological and folding-model potentials.[6]

As it can be seen from the above-mentioned studies,[4,5] most of the theoretical analyses for the scattering of deuterons and α particles from ^{9}Be targets have been performed using phenomenological potentials of the Woods–Saxon (WS) type. Therefore, in this paper, we aim to investigate the validity of the microscopic double-folding (DF) potential model to explain the elastic scattering of ^{3}He from ^{9}Be within the framework of the optical model.

This paper is part of our extensive study of the cluster structure of the ^{9}Be nucleus[7,8] and is devoted to analyze data on elastic and inelastic scattering of ^{3}He from ^{9}Be at energies E(^{3}He) = 30 MeV, 40 MeV and 47 MeV within various theoretical models.

The paper is organized as follows. In Sec. 2, the experimental procedure is given and in Sec. 3, the method used for the theoretical analysis of the experimental data is presented. Section 4 is devoted to the results of the experimental data, their theoretical analysis and discussion. The summary is given in Sec. 5.

2. Experimental Details

Experimental angular distributions of elastic and inelastic scattering of ^{3}He from ^{9}Be were measured using the extracted beams of isochronous cyclotron U-120 at the Nuclear Physics Institute (Řež, Czech Republic) at E(^{3}He) = 30, 47 MeV and K-130 cyclotron of the Jyväskylä University (Jyväskylä, Finland) at E(^{3}He) = 40 MeV. The average beam current during the experiments was maintained at 10 nA. The thickness of the self-supporting Be target was 12 μm. Peaks due to carbon and oxygen contaminations of the target were not observed in the energy spectra.

To measure (in)-elastically scattered ions, four Si–Si(Li) telescopes, each consisting of two ΔE_0, ΔE pin-diode detectors and silicon drift E_r detector with thicknesses of 10 μm, 100 μm and 3 mm, respectively, were used. To detect reaction products within a narrow angular opening, the telescopes were mounted at a distance of $\sim$ 25 cm from the target. Each telescope was shielded by a Cu–Pb collimator which has a total thickness of 5 mm and a circular hole of 3 mm diameter. Particle identification was based on the measurements of the energy-loss ΔE and

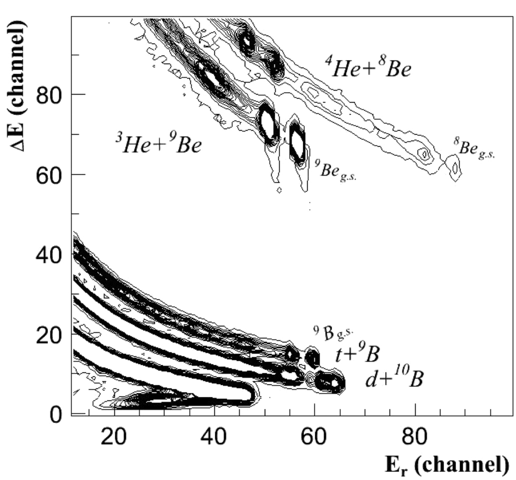

Fig. 1. Particle identification plot for the products of the ^{3}He+^{9}Be reaction measured at 47 MeV: d, tritium (t) and ^{4}He. ΔE is the energy loss and E_r is the residual energy.

residual energy E_r (the so-called ΔE-E method). The present detector system is similar to the one which we used before.[7]

The telescopes were mounted on rotating supports, which allowed to obtain data from $\theta_{\mathrm{lab}} = 20^\circ$ to 107° in steps of 1–2°. A two-dimensional plot of the energy loss ΔE versus the residual energy E_r is shown in Fig. 1. The good energy resolutions (full width half-maximum was about 150 keV) of both ΔE and E_r detectors allowed unambiguous identification of A and Z of each product.

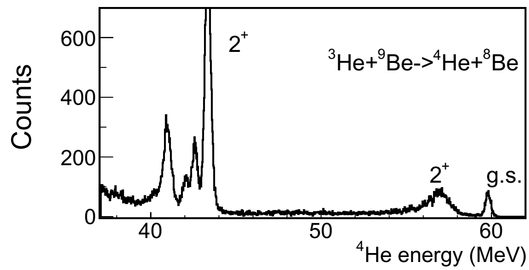

(a)

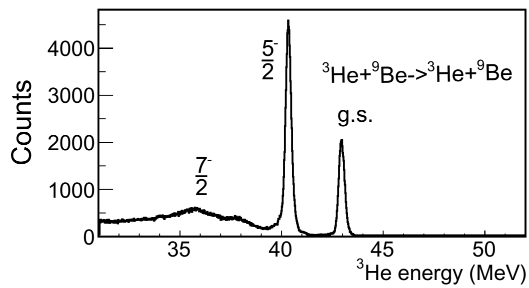

(b)

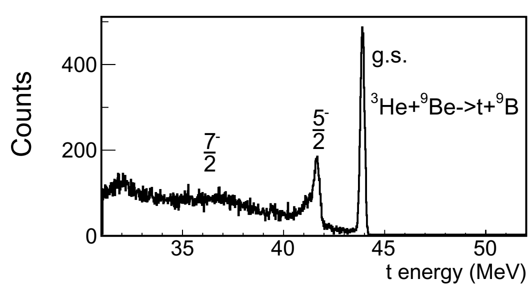

(c)

Fig. 2. Spectra of total deposited energy for the detected ^{4}He (a), ^{3}He (b) and t (c) at 24° in the laboratory system, for the reaction $^3\mathrm{He} + {}^9\mathrm{Be}$ at 47 MeV. The values were calculated as sum of the calibrated energy losses in two thin (10 and 100 μm) ΔE and residual energy E_r. The most populated excited states of ^{8}Be, ^{9}Be and ^{9}B, as well as populated ground states in the reaction channels $^9\mathrm{Be}(^3\mathrm{He}, {}^4\mathrm{He})^8\mathrm{Be}$ (a),$^9\mathrm{Be}(^3\mathrm{He}, {}^3\mathrm{He})^9\mathrm{Be}$ (b) and $^9\mathrm{Be}(^3\mathrm{He}, \mathrm{t})^9\mathrm{B}$ (c) were unambiguously identified.

This experimental technique allows us to identify the particles d, t, ^{3}He and ^{4}He, and to determine their total deposited energies. The spectra of total deposited energy are shown in Fig. 2. All peaks, which can be observed in the histograms in Fig. 2, were identified and found to belong to the ground and excited states of ^{9}Be, ^{9}B and ^{8}Be, as the complementary products to the detected particles ^{3}He, t and ^{4}He, respectively. Thus, the used technique allowed us to identify the reaction channel, to measure the energy of the products and to obtain differential angular distributions for various reaction channels.

3. Theoretical Calculations

The theoretical optical-model calculations for the elastic scattering data of ^{3}He from ^{9}Be target obtained from the literature[9,10] at energies 50 MeV and 60 MeV and for our data at the energies 30, 40 and 47 MeV were performed with the FRESCO[11] code using two approaches: (a) phenomenological optical potential and (b) semi-microscopic double-folding potential.

3.1. *Optical-model (OM) calculations: Phenomenological analysis*

The standard optical model with folding-model potentials or with similar phenomenological potentials such as the WS has failed to describe certain aspects of the experimental data, in particular the inelastic scattering data. Therefore, in the present calculations, we use volume-type real and imaginary potentials.[12,13] The full potential consists of the nuclear (V_{nucl}), spin-orbit (V_{so}) and the Coulomb (V_C) potentials.

$$U(r) = V_{\text{nucl}}(r) + V_{\text{so}}(r)(\overline{ls}) + V_C(r), \tag{1}$$

where the nuclear potential is assumed to have a WS shape:

$$V_{\text{nucl}}(r) = V_0\left[1+\exp\left(\frac{r-R_v}{a_v}\right)\right]^{-1} + iW\left[1+\exp\left(\frac{r-R_w}{a_w}\right)\right]^{-1}. \tag{2}$$

the spin-orbit potential is:

$$V_{\text{so}}(r) = V_0^{\text{so}}\left(\frac{1}{r}\right)\frac{d}{dr}\left[1+\exp\left(\frac{r-R_{\text{so}}}{a_{\text{so}}}\right)\right]^{-1}. \tag{3}$$

In addition, a Coulomb potential of a uniformly charged sphere is used:

$$V_C(r) = \frac{Z_p Z_t e^2}{2R_C}\left(3-\frac{r^2}{R_c^2}\right), \quad \text{for } r \le R_C$$

$$V_C(r) = \frac{Z_p Z_t e^2}{r}, \quad \text{for } r > R_C$$

with radius

$$R_i = r_i\left(A_p^{\frac{1}{3}} + A_t^{\frac{1}{3}}\right), \quad i = V, W, SO, C$$

Here, V_0 is the WS potential depth, R the potential radius and a the diffuseness parameter, which determines the sharpness of the potential surface. Z_p and Z_t are the proton numbers of the projectile and target of system, respectively.

3.2. *Optical-model calculations: Double-folding analysis*

The microscopic nuclear potential that we have also used to analyze the experimental data for the $^3\mathrm{He} + {}^9\mathrm{Be}$ system was based on the DF model.[14] The DF potential is calculated by using the nuclear-matter distributions of both projectile and target nuclei together with an effective nucleon–nucleon interaction potential (ν_{NN}). Thus, the DF potential is

$$V^{\mathrm{DF}}(R) = \int d\mathbf{r}_1 \int d\mathbf{r}_2 \rho_p(\mathbf{r}_1)\rho_t(\mathbf{r}_2)\nu_{\mathrm{NN}}(\mathbf{r}_{12}), \tag{4}$$

where $\rho_p(\mathbf{r}_1)$ and $\rho_t(\mathbf{r}_2)$ are the nuclear matter density distributions of both the projectile and target nuclei, respectively. Gaussian density distributions (GD) have been used for both nuclei[15,16] defined as:

$$\rho(r) = \rho_{(0)}\exp(-\beta r^2), \tag{5}$$

where β is adjusted to reproduce the experimental values for the root-mean-square radii of ^{3}He (1.91 fm) and ^{9}Be (2.51 fm).[17] $\rho_{(0)}$ values can be obtained from the normalization condition

$$\int \rho(r) r^2 dr = \frac{A}{4\pi}, \tag{6}$$

where A is the mass number. In order to reproduce elastic scattering data, $V^{\mathrm{DF}}(R)$ is usually multiplied by a free normalization factor, N_r.

The effective nucleon–nucleon interaction, ν_{NN}, is integrated over both density distributions. Several nucleon–nucleon interaction expressions can be used for the folding-model potentials. We have chosen the most common one, the M3Y (Michigan-3-Yukawa) realistic nucleon–nucleon interaction. The M3Y has two forms, one corresponds to M3Y-Reid[18] interaction and another is based on the so-called M3Y-Paris interaction.[19] In the present work, we use the former form with the relevant exchange correction term due to the Pauli principle, given by

$$\nu_{\mathrm{NN}}(r) = 7999\frac{\exp(-4r)}{4r} - 2134\frac{\exp(-2.5r)}{2.5r} + J_{00}(E)\delta(r)\mathrm{MeV}, \tag{7}$$

where $J_{00}(E)$ represents the exchange term, since nucleon exchange is possible between the projectile and the target. $J_{00}(E)$ has a linear energy dependence and can be expressed as

$$J_{00}(E) = 276\left[1 - 0.005\frac{E_{\mathrm{lab}}}{A_p}\right]\mathrm{MeVfm}^3. \tag{8}$$

In this case, while the real part of the optical-model potential has been obtained by using the above-described DF model, we have adopted the following WS form for the imaginary potential

$$W(r) = W_0 \left[1 + \exp\left(\frac{r - R_w}{a_w}\right)\right]^{-1}. \tag{9}$$

Therefore, for the nucleon–nucleon DF potential case, the nuclear potential consists of a real part and an imaginary part:

$$U^{\mathrm{DF}}(r) = N_r V_{\mathrm{DF}}(r) + iW(r), \tag{10}$$

where N_r is the normalization factor.

Theoretical calculations were carried out using the FRESCO code.

The phenomenological approach undoubtedly has simplicity, clarity, and convenience of application. However, it is well known that optical-potential parameters, which can describe experimental data in a wide energy range for various colliding nuclei, are often not unique. It is a rather complex problem, which leads to uncertainties in the choice of parameters of the interaction potential.

The volume integral J of the nuclear potential is a key value in the classification of various sets of potential parameters. Volume integrals assist in choosing a potential from a discrete set.

The optical WS and DF potentials can be conveniently characterized by real (J_V) and imaginary (J_W) volume integrals per nucleon

$$J_V = -\frac{4\pi}{A_p A_t}\int_0^\infty V(r) r^2 dr, \tag{11}$$

$$J_W = -\frac{4\pi}{A_p A_t}\int_0^\infty W(r) r^2 dr. \tag{12}$$

3.3. *Coupled-channel method*

The CC method implemented in FRESCO code has been used in data analysis for the excited states at different energies. The potential parameter set which can best describe elastic scattering was used in the CC calculations for the excited states. In CC calculations, we need to provide the code with some information about the concerned state (such as spin, parity, excitation energy) and also deformation parameter (β). In Sec. 4, we present deformation parameters for ^{9}Be states, which were used in the calculations for inelastic scattering in the method of coupled channels.

4. Results and Discussion

The comparison between the experimental data and the theoretical predictions for ^{9}Be(^{3}He, ^{3}He)^{9}Be at the aforementioned energies is shown in Fig. 3 based on the potential parameters, which are listed in Table 1. The error bars shown in Figs. 3 and 5 are mainly attributed to the statistical uncertainties, which are about 2–3%. In Fig. 3, the abbreviation WS corresponds to the calculations with a WS potential.

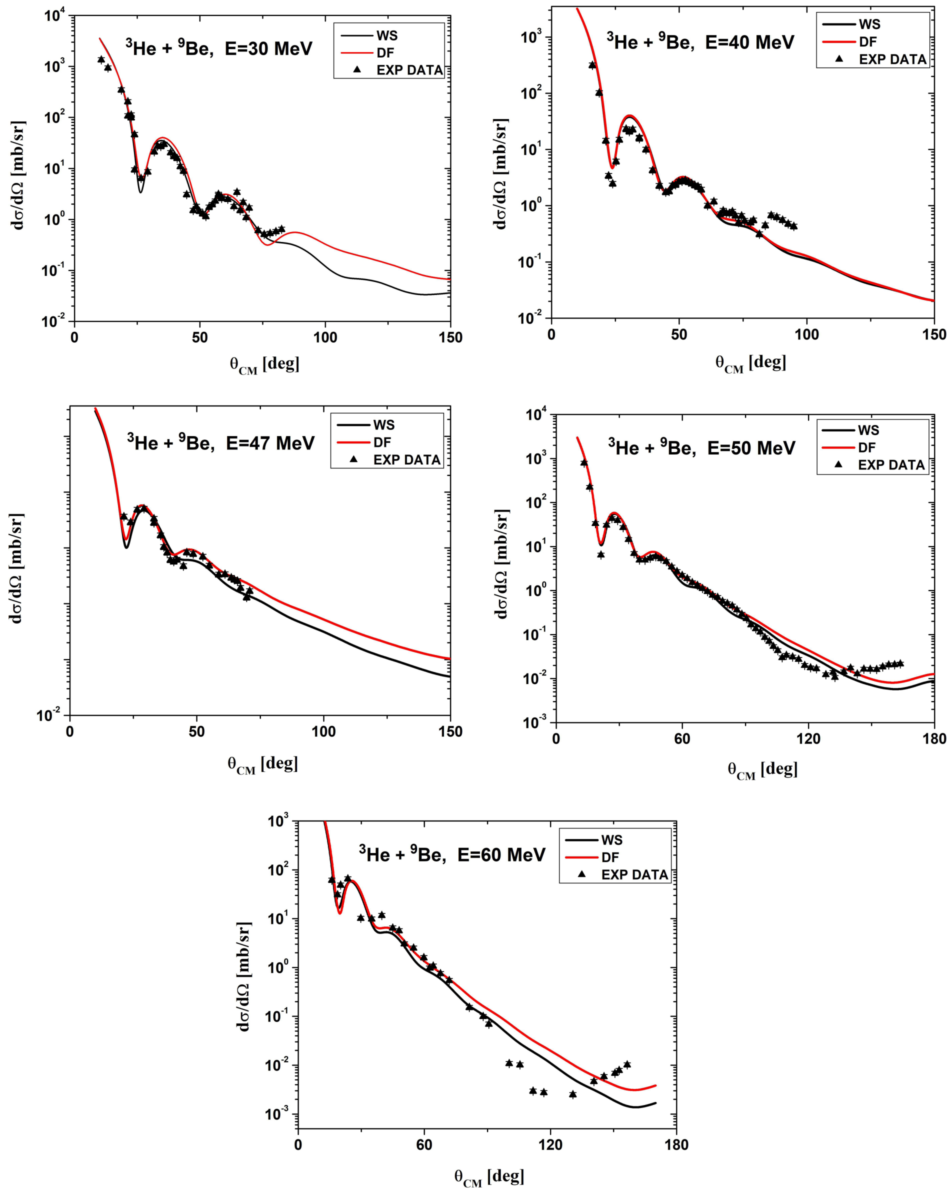

Fig. 3. Comparison of the experimental data and the calculated differential cross-sections for elastic scattering of ^{3}He from ^{9}Be at energies 30, 40, 47, 50 and 60 MeV using WS and DF potentials.

DF corresponds to the calculations with a folding-model potential for the real part and WS for the imaginary part.

One of the starting potentials was taken from Ref. 20, in which empirical expressions were proposed for a central potential with purely surface absorption, of which

Table 1. Potential parameters obtained for elastic scattering of ^{3}He from ^{9}Be at corresponding beam energies.

E (MeV)	Model	V (MeV)	r_V (fm)	a_V (fm)	N_r	W (MeV)	r_W (fm)	a_W (fm)	V_{so} (MeV)	r_{so} (fm)	a_{so} (fm)	χ^2/N
30	WS	75.43	1.255	0.821		23.03	1.57	0.91	6.76	1.07	0.66	3.99
	DF				1.2	23.03	1.57	0.91	6.76	1.07	0.66	9
40	WS	68.43	1.255	0.821		25.03	1.57	0.91	5.76	1.07	0.66	15.2
	DF				0.9	25.03	1.57	0.91	5.76	1.07	0.66	14.3
47	WS	63.43	1.265	0.821		19.03	1.57	0.91	5.06	1.07	0.66	7.58
	DF				1.09	19.03	1.57	0.91	5.06	1.07	0.66	9.54
50	WS	60.43	1.265	0.821		23.03	1.57	0.91	5.06	1.07	0.86	13
	DF				0.92	23.03	1.57	0.91	5.06	1.07	0.86	28
60	WS	58.43	1.265	0.821		26.03	1.57	0.91	3.66	1.07	0.66	49
	DF				0.93	26.03	1.57	0.91	3.66	1.07	0.66	68

the values of the parameters depend on the ^{3}He energy and the mass of the target nucleus. Such a potential well describes the scattering of ^{3}He in the energy range from 10 MeV to 220 MeV on various target nuclei from beryllium to lead. The search for the optical-potential parameters was carried out by fitting the calculated angular distributions to the experimental data using the computer code FRESCO.

In order to remove the discrete ambiguity in determining the optical potential, the radii of the nuclear density distribution and diffuseness of the potential were fixed. In this case, the radii of the real part are $r_V = 1.255$ fm for 30 MeV, 40 MeV and $r_V = 1.265$ fm for 47 MeV, 50 MeV and 60 MeV; the radius of the imaginary part is $r_W = 1.57$ fm for all energies and the radius of the spin-orbit part is $r_{so} = 1.07$ fm. The parameters of diffuseness are $a = 0.821$ and 0.91 fm for the real and imaginary parts of the volume potential and $a = 0.66$ for the spin-orbit part. Variations of the remaining three parameters of the optical potential (V, W and V_{so}) were carried out by fitting the theoretical calculations to the experimental data with χ^2 minimization. In the WS calculations, the Coulomb radius $r_C = 1.3$ fm was taken.

In the DF calculations, the normalization coefficient (N_r) for the real part of the potential was selected in the range of 0.9–1.2.

As can be seen from Fig. 3, the parameters of both WS and DF optical potentials well describe the obtained experimental data in spite of the fact that ^{9}Be is a cluster nucleus. It should be noted that the data at 30, 40 and 47 MeV were measured up to $\sim 100°$. Therefore, we do not see the contribution of cluster configurations to the ^{9}Be scattering cross-section. For example, in the case of 50 MeV and 60 MeV, it is clear that at the backward angles contribution of the cluster transfer to the scattering cross-section should be taken into account. Within the framework of the optical model, it is difficult to describe the increase of cross-section at the backward angles.

On the other hand, the desire to determine the global optical parameters and their energy dependence in the studied energy range has led to the WS and DF parameter sets that cannot adequately describe the experimental data at the rear angles at 50 MeV and 60 MeV energies.

The χ^2 criterion does not always allow us to make an unambiguous choice of the set of potential parameters. As a rule, to obtain additional information from the reaction and for a more adequate and optimal description of the experimental data, various integral characteristics of the potential are introduced, such as volume integrals.

As is seen from Table 2, the volume integrals of the real part (J_V) normalized by the number of interacting pair of projectile and target nucleons are within 350–500 MeV fm^3. It is well known that this integral is well determined by the data, as a relatively small variation of one of the potential parameters can be compensated by a small readjustment of the other parameters (continuous ambiguity), while keeping the integral as a constant. Thus, the volume integral plays as the representative of a

Table 2. Volume integrals of the real part (J_V) of the potential at different energies.

E (MeV)	J_V(WS) (MeV fm^3)	J_V(DF) (MeV fm^3)
30	449	489
40	407	363
47	385	435
50	367	363
60	355	364

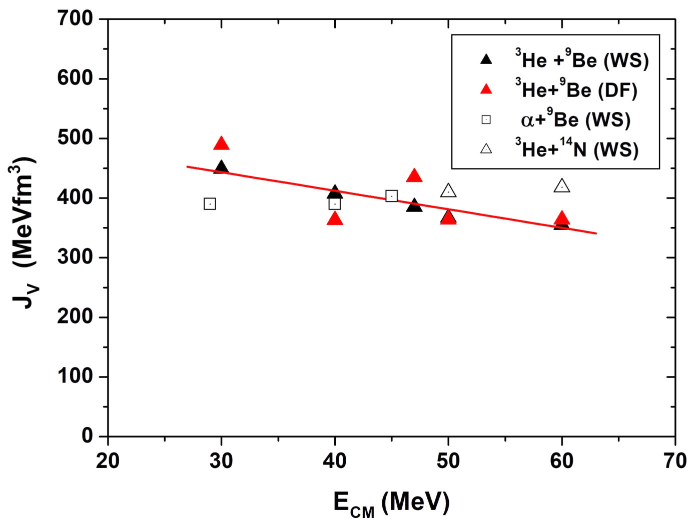

Fig. 4. (Color online) The energy dependence of volume integrals for the real J_V part of the WS (black triangle) and DF (red triangle) potentials for ^{3}He + ^{9}Be scattering. For comparison, volume integrals for the real J_V parts of potentials for $\alpha + {}^9$Be (empty square)[23] and ^{3}He +^{14} N (empty triangle)[24] scattering are presented.

given family of potentials. For interaction of ^{3}He and α particles with 1p-shell nuclei at an incident beam energy of several tens of MeV, it is found that the reasonable value of the volume integral is $J_V \sim 400\,\mathrm{MeV\ fm}^3$. This follows from the predictions of the microscopic theory (folding model) and phenomenological data analysis of the elastic scattering in the energy range from 10 MeV to 200 MeV.[20–23] Volume integrals for the real part of optical potential were calculated[23] for $\alpha+{}^9$Be system at energies close to the energies considered in this paper. The volume integrals (J_V) for WS and DF potentials calculated in this work are within the same range. Figure 4 shows the calculated volume integrals for $^3\mathrm{He} + {}^9\mathrm{Be}$, $\alpha + {}^9\mathrm{Be}$[23] and $^3\mathrm{He} + {}^{14}\mathrm{N}$[24] systems, depending on the energy.

Inelastic scattering off light nuclei is of interest from two points of view. Firstly, the structure of the low-lying states is sufficiently well known which is important for the analysis, and secondly, the level density is not high, thus permitting the measurement of differential cross-sections even with a modest energy resolution.

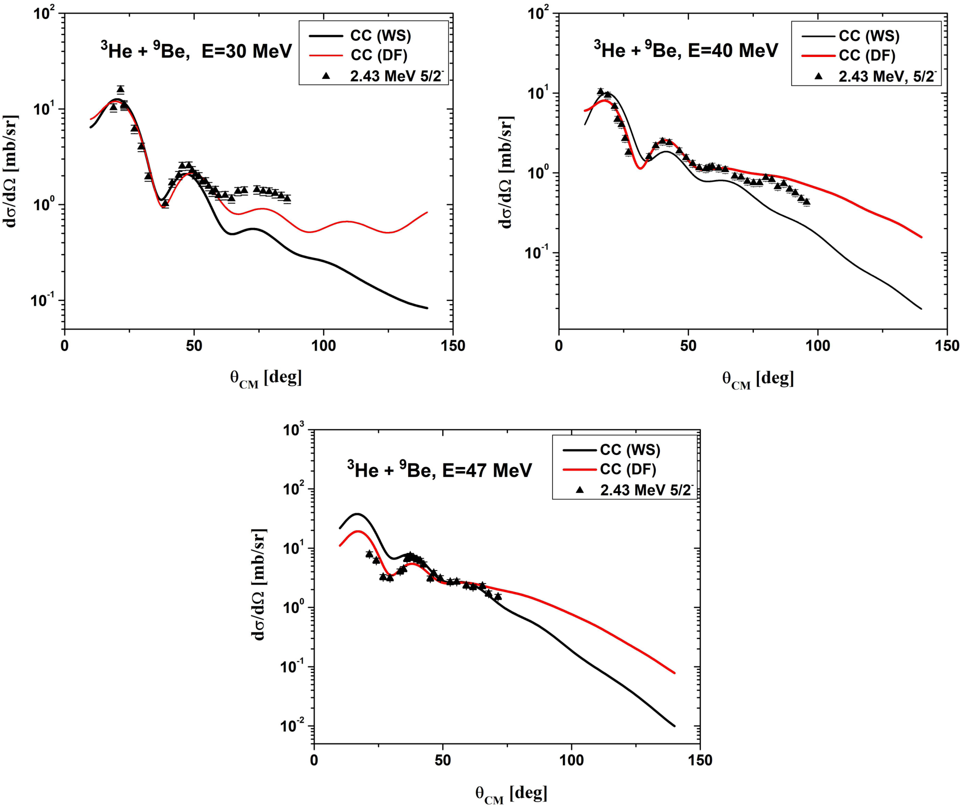

Fig. 5. Comparison between the experimental data and the calculated differential cross-sections for inelastic scattering of ^{3}He from ^{9}Be (2.43 MeV $(5/2^-)$) at different energies using different potentials in CC method: WS and double folding.

Table 3. Deformation parameters of the excited 2.43 MeV ($5/2^-$) state of ^{9}Be.

E (MeV)	Potential in CC method	β ($5/2^-$)
30	WS	0.80
	DF	0.80
40	WS	0.78
	DF	0.78
47	WS	0.80
	DF	0.80

The resulting optical potentials were used to calculate the differential cross-sections for inelastic scattering in the context of the CC method. The cross-sections for the excitation of the low-lying state at 2.43 MeV ($5/2^-$) belonging to the rotational band in the ^{9}Be nucleus were calculated. In the calculations, we used the WS potential (CC (WS)) and DF potential (CC (DF)) from Table 1.

The comparison between the experimental data and theoretical predictions for the state at 2.43 MeV ($5/2^-$) at energies E(^{3}He) = 30 MeV, 40 MeV and 47 MeV is shown in Fig. 5. The best description is obtained by using CC (DF) potential.

Analysis of inelastic scattering data within the CC approach allows one to extract the information on the deformation of an excited nucleus treating these states as collective rotational excitations. As mentioned above, in CC calculations we should provide parameters with information about the concerned state, such as spin, parity and excitation energy. ^{9}Be is a deformed nucleus. In our calculations of the inelastic scattering of ^{3}He from ^{9}Be at energies 30 MeV, 40 MeV and 47 MeV deformation parameters were used, which are in the range of 0.78–0.80. Deformation parameters of the excited state 2.43 MeV ($5/2^-$) of ^{9}Be nuclei at the indicated energies are shown in Table 3. They agree well with the data from other sources.[8,25,26]

5. Summary

We obtained new experimental data for elastic scattering and inelastic scattering populating the 2.43 MeV ($5/2^-$) excited state in ^{9}Be using ^{3}He beams at energies of 30, 40 and 47 MeV incident on a ^{9}Be target. The data on elastic scattering were analyzed using two approaches: usual optical-model potential (phenomenological) and double-folding potential (semi-microscopic). Additionally, we apply our data analysis to the previous measurements at higher energies. The volume integrals of the deduced real potentials are within the 350–500 MeV fm^3 interval, which is consistent with the predictions of the microscopic theory and with the results of the global analysis of the elastic scattering of α particles and ^{3}He in the 10–200 MeV energy range. The data for the excited state were analyzed within the framework of the coupled-channel method with two different potentials: WS and double-folding potentials. The obtained deformation parameters for the ^{9}Be nucleus at 30 MeV, 40 MeV and 47 MeV are close to the results obtained in Refs. 8, 25 and 26.

We plan to analyze the experimental data for transfer reactions induced by the $^3\mathrm{He} + {}^9\mathrm{Be}$ system, with exit channels such as $\alpha + {}^8\mathrm{Be}$, $\mathrm{t} + {}^9\mathrm{B}$ and $^5\mathrm{He} + {}^7\mathrm{Be}$, using the present optical-potential parameters in future.

Acknowledgments

The work was supported by the Russian Science Foundation (17-19-01170), the CANAM (IPN ASCR), by the grants to JINR (Dubna) from the Czech Republic, the Republic of Poland and the mobility grant from the Academy of Finland. We would like to thank the JYFL Accelerator Laboratory (Jyväskylä), Finland and NPI (Řež) for giving us the opportunity to perform this study as well as the cyclotron staff of both institutes for the excellent beam quality.

References

1. A. S. Demyanova *et al.*, *JETP Lett.* **102**(7) (2015) 413.
2. N. Burtebayev *et al.*, *Int. J. Mod. Phys. E* **27**(3) (2018) 1850025.
3. A. S. Demyanova *et al.*, *EPJ Web Conf.* **66** (2014) 02027.
4. S. Tanaka *et al.*, *J. Phys. Soc. Japan* **45**(3) (1978) 733.
5. M. N. Harakeh *et al.*, *Nucl. Phys. A* **344** (1980) 15.
6. S. Roy *et al.*, *Phys. Rev. C* **52** (1995) 1524.
7. S. M. Lukyanov *et al.*, *J. Phys. G: Nucl. Part. Phys.* **41** (2014) 035102.
8. B. A. Urazbekov *et al.*, *Bull. Rus. Acad. Sc.*: *Phys.* **81**(6) (2017) 690.
9. N. Burtebayev *et al.*, *Conf. Nucl. Science & Appl., Izmir* **2000** (2000) 822.
10. A. T. Rudchik *et al.*, *Nucl. Phys. A* **609** (1996) 147.
11. I. J. Thompson, *Comput. Phys. Rep.* **167** (1988) 7.
12. Y. Kucuk and I. Boztosun, *Nucl. Phys. A* **764** (2006) 160.
13. M. Freer *et al.*, *Phys. Rev. C* **76** (2007) 034320.
14. J. Cook, *Comput. Phys. Comm.* **25** (1982) 125.
15. M. Karakoc and I. Boztosun, *Phys. Rev. C* **73** (2006) 047601.
16. M. Aygun *et al.*, *Nucl. Phys. A* **848** (2010) 245.
17. H. de Vries, C. W. de Jager and C. de Vries, *At. Data Nucl. Data Tables* **36** (1987) 495.
18. G. Bertsch *et al.*, *Nucl. Phys. A* **284** (1977) 399.
19. N. Anantaraman, H. Toki and G. F. Bertsch, *Nucl. Phys. A* **398** (1983) 269.
20. H. Trost, P. Lezoch and U. Strohbusch, *Nucl. Phys. A* **462** (1987) 333.
21. H. Abele *et al.*, *At. Nucl.* **15** (1987) 373.
22. R. Grgen *et al.*, *Nucl. Phys. A* **320** (1979) 296.
23. A. H. Amer *et al.*, *Int. J. Chem. Mol. Nucl. Mater. Metal. En.* **10** (2016) 129.
24. N. Burtebayev *et al.*, *Act Phys. Pol. B* **47** (2016) 2017.
25. W. Fitz, R. Jahr and R. Santo, *Nucl. Phys. A* **101** (1967) 449.
26. A. Szczurek *et al.*, *Z. Phys. A* **333** (1989) 271.